

Original Research

# C3aR Antagonist Alleviates C3a Induced Tubular Profibrotic Phenotype Transition via Restoring PPAR $\alpha$ /CPT-1 $\alpha$ Mediated Mitochondrial Fatty Acid Oxidation in Renin-Dependent Hypertension

Chongjian Wang<sup>1,†</sup>, Zhiyu Wang<sup>1,†</sup>, Jing Xu<sup>1</sup>, Hongkun Ma<sup>1</sup>, Kexin Jin<sup>1</sup>, Tingting Xu<sup>1</sup>, Xiaoxia Pan<sup>1</sup>, Xiaobei Feng<sup>1</sup>, Wen Zhang<sup>1,\*</sup><sup>1</sup>Department of Nephrology, Ruijin Hospital, Shanghai Jiao Tong University School of Medicine, Shanghai 200025, China\*Correspondence: [zhangwen255@163.com](mailto:zhangwen255@163.com) (Wen Zhang)

†These authors contributed equally.

Academic Editor: Natascia Tiso

Submitted: 29 May 2023 Revised: 22 July 2023 Accepted: 25 July 2023 Published: 17 October 2023

## Abstract

**Background:** Renin-dependent hypertension with tubulointerstitial injury remains a problem with high prevalence in the clinic. However, whether and how renin participates in tubulointerstitial injury remains incompletely understood. New evidence suggests that renin cleaves C3 into C3a and C3b. In the present study, we aimed to explore the role of renin-mediated C3a/C3a receptor (C3aR) signaling in renin-dependent hypertension-induced kidney injury and illustrate the detailed mechanisms. **Methods:** C3a concentration changes in serum from healthy volunteers incubated with recombinant renin were detected by ELISA. C3aR expression in human tubular epithelial cells was evaluated in renal biopsy sections from malignant arteriolonephrosclerosis and benign arteriolonephrosclerosis patients. C3aR changes in human kidney 2 (HK2) cells were detected after the cells were treated with human serum, renin and aliskiren. The C3a analogue and C3aR antagonist SB290157 were used to stimulate HK2 cells to explore the downstream signaling of C3a/C3aR activation. For *in vivo* studies, two-kidney, one-clipped (2K1C) hypertensive rat model was established to simulate renin-dependent hypertension conditions. C3a and C3aR expression was detected in the clipped kidneys. SB290157 was injected intraperitoneally to block C3a/C3aR signaling in 2K1C rats. **Results:** The results showed that renin cleaved C3 into C3a and activated C3a/C3aR signaling in tubular epithelial cells (TECs) from both humans and rats. *In vitro* results demonstrated that C3a/C3aR activation impaired peroxisome proliferator-activated receptor alpha (PPAR $\alpha$ )/carnitine palmitoyltransferase-1 alpha (CPT-1 $\alpha$ )-mediated mitochondrial fatty acid oxidation (Mito FAO) in HK2 cells and induced HK2 cell transition to a profibrotic phenotype, which was inhibited by treatment with the C3aR antagonist SB290157. *In vivo* results showed that renin mRNA levels, C3a concentrations, C3aR levels and tubulointerstitial fibrosis increased concurrently in the clipped kidney cortex of 2K1C rats. Treatment with the C3aR antagonist SB290157 significantly mitigated the effect of renin induction of C3aR expression and alleviated renin-dependent hypertension-induced tubulointerstitial fibrosis by improving PPAR $\alpha$ /CPT-1 $\alpha$ -mediated Mito FAO in TECs, as well as inhibiting tubular profibrotic phenotype transition. **Conclusions:** Our results prove that renin activates C3a/C3aR signaling to promote renal tubulointerstitial fibrosis by impairing PPAR $\alpha$ /CPT-1 $\alpha$ -mediated tubular Mito FAO. SB290157 confers a potential therapeutic approach for renin-dependent hypertension-induced kidney injury.

**Keywords:** hypertension-induced kidney injury; renin; C3a; C3a receptor; mitochondrial fatty acid oxidation; profibrotic phenotype transition

## 1. Introduction

Hypertension is one of the most common causes of secondary kidney diseases and a major contributor to chronic renal dysfunction [1,2]. Overactivation of the sympathetic nervous system [3] or renal artery stenosis [4] leads to low renal blood flow and subsequently increased renin secretion from the juxtaglomerular apparatus, which result in renin-dependent hypertension. Recently, a curious relationship among the renin-angiotensin system (RAS), immune activation and tubular injury is highlighted [5]. New evidence suggests that renin can cleave C3 to produce C3a and C3b, and the application of renin inhibitors reduces renin-induced C3 cleavage and mitigates tubulointerstitial injury [6,7]. However, the mechanisms by which renin affects tubulointerstitial injury are not fully understood.

Complement C3, as the central molecule of the complement system, has been implicated in the pathogenesis of several chronic kidney diseases (CKDs) [8–10]. Reportedly, C3 and its cleavage fragments accumulate in the glomerular capillaries and arterioles of the kidneys in patients with hypertension [11]. The intensity of C3 deposition is associated with the severity of hypertension-induced kidney injury [12,13]. Apart from serum-derived C3 deposition, local synthesis of C3 under disease conditions also contributes to renal damage [14]. C3a, the smaller cleavage fragment of C3, can regulate intracellular signaling by binding to the C3a receptor (C3aR), which is located on the cellular membrane [15]. In the kidney cortex, C3aR is mainly expressed in tubular epithelial cells (TECs) and interstitial infiltrating immune cells such as



monocytes and macrophages [16,17]. Evidence has revealed that C3a/C3aR signaling plays a vital role in renal tubulointerstitial fibrosis in several CKD models, such as unilateral ureteral obstruction model and adriamycin-induced proteinuria model, by promoting tubular profibrotic phenotype transition and mesenchymal transition [18–20]. In addition, C3aR inhibition has been reported to be a promising treatment to alleviate tissue fibrosis in different disease models [21,22]. However, the effect of renin-induced C3a/C3aR signaling on the renal tubulointerstitium and the effect of C3aR antagonist on renin-dependent hypertension-induced kidney injury have not been fully elucidated. Studies suggest that hypertension suppresses peroxisome proliferator-activated receptor alpha (PPAR $\alpha$ )-mediated lipid metabolism in TECs, resulting in abnormal lipid accumulation and aggravating the development of hypertension-induced tubulointerstitial injury [23]. The activation of C3a/C3aR signaling has been reported to modulate lipid metabolism in different types of cells [24,25]. Nevertheless, whether renin/C3a/C3aR signaling promotes hypertension-induced kidney injury by impairing PPAR $\alpha$ -mediated lipid metabolism remains unknown.

Here, we conducted *in vitro* and *in vivo* experiments to simulate the renin-dependent hypertension-induced kidney injury microenvironment to explore how renin/C3a/C3aR signaling regulates renal tubulointerstitial injury and illustrates whether the C3aR antagonist SB290157 can protect against renin-dependent hypertension-induced kidney injury by restoring mitochondrial fatty acid oxidation (Mito FAO) and mitigating mesenchymal transition through C3a/C3aR signaling.

## 2. Materials and Methods

### 2.1 Incubation of Volunteer Serum with Recombinant Human Renin

Serum samples collected from seven healthy volunteers were stored in aliquots at  $-80^{\circ}\text{C}$ . After a 1:10 dilution in Dulbecco's phosphate-buffered saline (DPBS, Gibco, Waltham, MA, USA), serum samples were incubated with recombinant renin (1.2  $\mu\text{g}/\text{mL}$ , BioVision, Waltham, MA, USA) or phosphate-buffered saline (PBS, Gibco) at  $37^{\circ}\text{C}$  for 24 h. After incubation, the C3a level of the samples was detected immediately with a Complement C3a Human ELISA Kit (Thermo Scientific, Waltham, MA, USA) according to the manufacturer's instructions.

### 2.2 HK2 Cells Culture and Stimulation

Immortalized human tubular epithelial cells (human kidney 2 (HK2) cells, CRL-2190, ATCC, Manassas, VA, USA) were routinely cultured in Dulbecco's modified Eagle's medium/nutrient mixture F-12 (DMEM/F12, Gibco) containing 10% fetal bovine serum (FBS, Gibco) as described previously [26]. The cell lines were mycoplasma-free (Mycoplasma Detection Kit, Yeasen, Shanghai, China) and authenticated by STR identification.

HK2 cells were treated with 10% serum from healthy volunteer 7 (H7) supplemented with recombinant renin (1.2  $\mu\text{g}/\text{mL}$ ) or PBS at  $37^{\circ}\text{C}$  for 24 h. Aliskiren (10  $\mu\text{M}$ , MedChemExpress, Monmouth Junction, NJ, USA), a specific renin inhibitor, was preincubated with recombinant renin for 1 h before addition.

A C3a analogue, which has been reported to mimic the natural biological activity of C3a [27,28], was used to explore the effect of C3a/C3aR activation. HK2 cells were treated with the C3a analogue (1  $\mu\text{g}/\text{mL}$ , Sangon Biotech, Shanghai, China) or PBS for 24 h. For C3aR inhibition, cells were pretreated with the C3aR antagonist SB290157 (1  $\mu\text{M}$ , Sigma–Aldrich, St. Louis, MO, USA) for 1 h. HK2 cells were harvested for western blotting analysis, and the culture medium was used to evaluate the concentration of transforming growth factor  $\beta$  (TGF $\beta$ ) using Human TGF $\beta$  ELISA kits (Proteintech, Wuhan, China) according to the manufacturer's instructions.

### 2.3 Immunocytochemistry (ICC) Staining

HK2 cells after the treatment were fixed in 4% paraformaldehyde and permeabilized in 0.2% Triton X-100, followed by incubation with 2% BSA for 1 h. The cells were then incubated with PPAR $\alpha$  antibodies (1:100, Thermo Scientific) at  $4^{\circ}\text{C}$  overnight and subsequently with the Alexa Fluor $^{\text{®}}$  488-conjugated secondary antibody (1:500, Abcam, Discovery Drive, Cambridge, UK) at  $37^{\circ}\text{C}$  for 45 min. DAPI (1:1000, Sigma–Aldrich) was used to counterstain cellular nuclei. The cells were observed under a fluorescence microscope. The intensity of PPAR $\alpha$  fluorescence was quantified using ImageJ (version 1.51, National Institutes of Health, Bethesda, MD, USA).

### 2.4 Detection of Free Fatty Acid and Mitochondria

The fatty acid uptake probe in the Fatty Acid Uptake Assay Kit (Dojindo Laboratories, Kamimashiki-gun, Kumamoto, Japan) functions as a fatty acid analogue and shows the cellular uptake capacity of fatty acids directly. MitoBright LT Deep Red (Dojindo Laboratories) can mark the mitochondria. HK2 cells completing the treatment were stained with the fatty acid probe and subsequently with MitoBright LT Deep Red. The cells were observed by confocal microscopy (LSCM, LSM800, Zeiss, Oberkochen, Germany). The colocalization between the fatty acid probe and MitoBright LT Deep Red was measured by ImageJ with the Coloc 2 plugin and presented as Manders' coefficients.

### 2.5 Human Kidney Samples

Three patients with malignant arterionephrosclerosis (MANS) and three patients with benign arterionephrosclerosis (BANS) were included in this study. The study protocol was approved by the Ethics Committee of Ruijin Hospital, Shanghai Jiao Tong University School of Medicine. All of the kidney tissues were obtained from renal biopsies. Informed consent was obtained from all of the patients. Paraffin-embedded kidney sections were prepared for immunofluorescence.

## 2.6 Incubation of the Rat C3 Protein with Recombinant Rat Renin

Recombinant rat renin protein (active) (Abcam) and rat C3 protein (Complement Technology, Tyler, TX, USA) were used in the experiment. Purified rat C3 protein (100 µg/mL) was incubated with recombinant rat active renin at concentrations of 0, 1.2, 12.5, and 25 µg/mL at 37 °C for 24 h. After incubation, the sample was mixed with 5× loading buffer (Beyotime, Shanghai, China) and boiled for 10 min. Samples with equal volume were used to conduct western blotting analysis to detect the cleavage fragment of C3.

## 2.7 Animals and Two-Kidney, One-Clipped (2K1C) Rat Hypertension Model

Male Sprague–Dawley (SD) rats weighing 150–170 g were purchased from Charles River Laboratories (Beijing, China) and housed at optimal temperature (22 ± 2 °C) with a 12-hour light-dark cycle. The animal experiments were approved by the Animal Experiments Ethics Committee of Charles River Laboratories. Rats were acclimated to the housing conditions for 3 days prior to the experiments. For the 2K1C model, the rats were anesthetized with isoflurane (induction: 5%, maintenance: 2%), and the left kidney was exposed through a dorsal flank incision. A U-shaped silver clip with a 0.25 mm inner diameter (Alcott Biotech, Shanghai, China) was placed on the left renal artery. The same surgery was performed on the rats in the sham group but without the clip. The animals were sacrificed at 2 or 4 weeks after the surgery to collect plasma, serum and renal cortex tissue for further analysis.

## 2.8 C3aR Antagonist Treatment

The C3aR antagonist SB290157 was used to inhibit C3a/C3aR signaling activation *in vivo*. SB290157 was intraperitoneally injected into rats at a dose of 3 mg/kg per day for 4 weeks after the surgery. The nondrug-treated groups received an equal volume of vehicle at the same time.

## 2.9 Blood Pressure Measurement

The tail artery blood pressure of rats was measured at different time points (before the surgery and 2 weeks and 4 weeks after the surgery) using the BP-2000 Blood Pressure Analysis System (Visitech Systems, Apex, NC, USA). Prior to the measurement, all rats were acclimated in restraints. The blood pressure of each rat was determined by averaging 3 records.

## 2.10 Analysis of Plasma Renin, Plasma C3a and Kidney Tissue C3a Levels

Plasma samples were collected from rats using EDTA-coated Eppendorf tubes. The concentration of renin in plasma was measured using a Renin Assay Kit (Fluorometric) (Abcam). For acquiring kidney tissue homogenates, a piece of kidney cortex tissue from each sample was weighed. We added PBS (tissue weight (g): PBS volume (mL) = 1:9) and two beads to each vial containing the

sample and homogenized the tissue at 60 Hz for 30 s for three times with Tissue Grinders (Jingxin, Shanghai, China) to obtain tissue homogenates. The homogenates were centrifuged 5000 ×g at 4 °C for 10 min to obtain the supernatant. The concentrations of C3a in plasma and kidney tissue homogenates were measured using a Rat C3a ELISA Kit (Elabscience), according to the manufacturer's instructions.

## 2.11 Renal Function and Histology Analysis

The level of serum creatinine (Scr) was determined by using a liquid chromatography-tandem mass spectrometry (LC–MS/MS) method according to the manufacturer's instructions. The severity of tubular damage was assessed by two nephrologists in a blinded manner after observing whole kidney sections by hematoxylin-eosin (H&E) staining. Tubular damage was scored from 0 to 4 according to the distribution of lesions as follows: 0, no lesions; 1, less than 25%; 2, 25–50%; 3, 50%–75%; and 4, more than 75%. Renal tubulointerstitial fibrosis was quantified as the percentage of blue area per field in Masson's trichrome-stained sections using ImageJ, and ten fields of view for each sample were used to collect the data.

## 2.12 Western Blotting Analysis

The renal cortex tissue and cells were lysed in radioimmunoprecipitation assay (RIPA) buffer (Sigma–Aldrich) containing a protease/phosphatase inhibitor cocktail (NCM Biotech, Jiangsu, China). The protein concentration of the samples was measured with a bicinchoninic acid assay (BCA) protein quantitation kit (Beyotime). Equal amounts of protein (20 µg for cells and 30 µg for tissues) were separated via 10% sodium dodecyl sulfate-polyacrylamide gel electrophoresis (SDS-PAGE) and transferred to a polyvinylidene difluoride (PVDF) membrane. After incubation in fast blocking buffer (EpiZyme, Shanghai, China), the membrane was incubated with the following primary antibodies at 4 °C overnight: anti-C3aR (1:1000, Bioss, Beijing, China), anti-C3/C3b (1:2000, Abcam), anti-TGFβ (1:1000, Proteintech), anti-PPARα antibodies (1:1000, Thermo Scientific), anti-carnitine palmitoyltransferase-1α (CPT-1α, 1:5000, Proteintech), anti-α-smooth muscle actin (α-SMA, 1:4000, Sigma–Aldrich) and anti-GAPDH (1:5000, Proteintech). After 3 washes, the membranes were then incubated with horseradish peroxidase (HRP)-conjugated secondary antibodies (1:2500, Cell Signaling Technology, Danvers, MA, USA) at room temperature for 1 h. The visualized signal bands were measured using enhanced chemiluminescence (EpiZyme) through a chemiluminescence imaging system (Tanon, Shanghai, China). The intensity of the bands was determined with ImageJ. Target protein levels were normalized to GAPDH and expressed as fold change relative to the control group.

### 2.13 RNA Extraction, Reverse Transcription, and Quantitative Reverse Transcription PCR (RT-qPCR)

Total RNA from renal cortex tissues and cells was extracted using the FastPure Cell/Tissue Total RNA Isolation Kit (Vazyme, Jiangsu, China). Complementary DNA was generated using the HiScript® III 1st Strand cDNA Synthesis Kit (+gDNA wiper) (Vazyme), and qPCR was performed using the ChamQ Universal SYBR qPCR Master Mix (Vazyme). The specific primers used were as follows: Rat REN (F) GATCACCATGAAGGGGTCTCTGT (R) GTTCCTGAAGGGATTCTTTTGCAC; Rat C3aR (F) AGGCAATGGGCTGGTGTCTGT (R) CAGGAA-GACTGGCAAACAT; Rat  $\alpha$ -SMA (F) AC-CATCGGGAATGAACGCTT (R) CTGTCAGCAAT-GCCTGGGT; Rat TGF $\beta$  (F) ATACGCCTGAGTG-GCTGTCT (R) TGGGACTGATCCCATTTGATT; Rat CD68 (F) TGTTCACTCCAAGCCCAA (R) GCTCT-GATGTCGGTCCTGTTT; and Rat GAPDH (F) GC-CTTCCGTGTTCTTA (R) AGACAACCTGGTCCTCA. Data were expressed as an amplification number based on  $2^{-\Delta\Delta C_t}$  normalized to GAPDH and compared with controls.

### 2.14 Transmission Electron Microscopy (TEM)

The renal cortex tissues were cut into 1 mm<sup>3</sup> sections and fixed in 2.5% glutaraldehyde. The tissues were then fixed in 1% osmium tetroxide, dehydrated in a graded ethanol series, embedded in hard resin and sectioned into ultrathin slices (80 nm) using an ultramicrotome (Leica, Wetzlar, Germany). The slices were then stained with uranyl acetate and lead citrate before being observed. We focused on observing lipid droplets in tubular epithelial cells.

### 2.15 Immunofluorescence

The kidneys were fixed in 4% paraformaldehyde, embedded in paraffin and cut into 4- $\mu$ m-thick sections. After dehydration and antigen retrieval by EDTA (pH 9.0) under high temperature and high pressure, the kidney sections were then incubated with the following primary antibodies at 4 °C overnight: anti-E-cadherin (E-cad) antibody (1:4000, TSA, Proteintech), anti-C3aR antibody (1:100, Bioss), anti-CD68 antibody (1:200, Servicebio, Wuhan, China), anti- $\alpha$ -SMA antibody (1:200, Sigma-Aldrich), anti-PPAR $\alpha$  antibodies (1:100, Thermo Scientific) and anti-aquaporin 1 (AQP1) antibodies (1:200, Abcam). The kidney sections were then incubated with secondary antibodies at 37 °C for 45 min. For TSA staining, the sections were additionally incubated with FITC-tyramide solution protected from light for 10 min. DAPI was used to counterstain cell nuclei. The kidney sections were observed under a fluorescence microscope. The fluorescence intensity of C3aR, PPAR $\alpha$  and the CD68% positive area of each sample were determined by ImageJ. Five fields of view of each sample from patients and ten fields of view of each sample from rats were used for analysis. Fields of view at 200 $\times$  mag-

nification were located in the renal cortex and chosen randomly under the microscopy. After acquiring the images of the specific channel, the images were converted to an 8-bit image and the positive area was included by setting a certain threshold. After selecting “Limit to Threshold” option in the “Set Measurements”, the mean fluorescence intensity and the percentage of positive area could be quantified using ImageJ [29]. The fluorescence intensity of each sample was determined by averaging the data from five or ten images. The mean intensity of the control group in each experiment was used as a reference in the statistical analysis. The colocalization of PPAR $\alpha$  and nuclei was measured by ImageJ with the Coloc 2 plugin and presented as Manders’ coefficients.

### 2.16 Statistical Analysis

The distribution of data were examined by Shapiro-Wilk test. The values for each parameter were expressed as the mean  $\pm$  SEM. Statistical analysis were performed using GraphPad 8.0 (GraphPad Software, La Jolla, CA, USA). Two-tailed, unpaired Student’s *t* tests were used when comparing two groups. One-way ANOVA followed by Tukey’s multiple comparisons test was used to compare the differences between groups when there were more than two groups. Paired *t* tests were performed to analyze the differences between the serum-recombinant human renin incubation groups and the serum-PBS incubation groups. *p* < 0.05 was considered statistically significant.

## 3. Results

### 3.1 Recombinant Human Renin Increases the C3a Concentration in Human Serum

Serum from seven healthy volunteers was collected and incubated with recombinant human renin or PBS. As shown in Table 1, the C3a concentration in serum incubated with recombinant renin increased significantly compared to that in the same samples incubated with PBS (with renin  $922.16 \pm 312.90$  ng/mL vs. with PBS  $561.52 \pm 156.54$  ng/mL, *t* = 2.989, *p* = 0.024). The median level of  $\Delta$ C3a (C3a concentration with renin-C3a concentration with PBS) in these samples was 198.56 (134.46, 810.24) ng/mL.

### 3.2 Renin Induces C3a/C3aR Activation in Human Tubular Epithelial Cells

As C3aR is mainly expressed in TECs, we used serum from H7 incubated with human recombinant renin to stimulate HK2 cells and investigated the change in C3aR. As shown in Fig. 1A, treatment with serum incubated with recombinant renin significantly increased the protein level of C3aR in HK2 cells. The addition of aliskiren, a renin inhibitor, reversed the change in C3aR protein levels.

To further validate the results in human kidneys, we performed immunofluorescence staining of C3aR in kidney samples from 6 hypertensive patients who underwent renal biopsy. Among them, 3 were diagnosed with BANS

**Table 1. Comparison of C3a concentrations in serum samples from 7 healthy volunteers after incubation with recombinant human renin or PBS.**

Patient	C3a Concentration with PBS (ng/mL)	C3a Concentration with Renin (ng/mL)	$\Delta$ C3a Concentration (ng/mL)	t-value	p-value
H1	340.78	444.23	103.45	2.989	0.024*
H2	560.23	758.79	198.56		
H3	644.18	778.64	134.46		
H4	577.3	851.79	274.49		
H5	835.77	1006.8	171.03		
H6	534.45	1344.69	810.24		
H7	437.96	1270.15	832.19		

$\Delta$ C3a concentration = C3a concentration with renin - C3a concentration with PBS; \* $p < 0.05$  by paired  $t$  test.

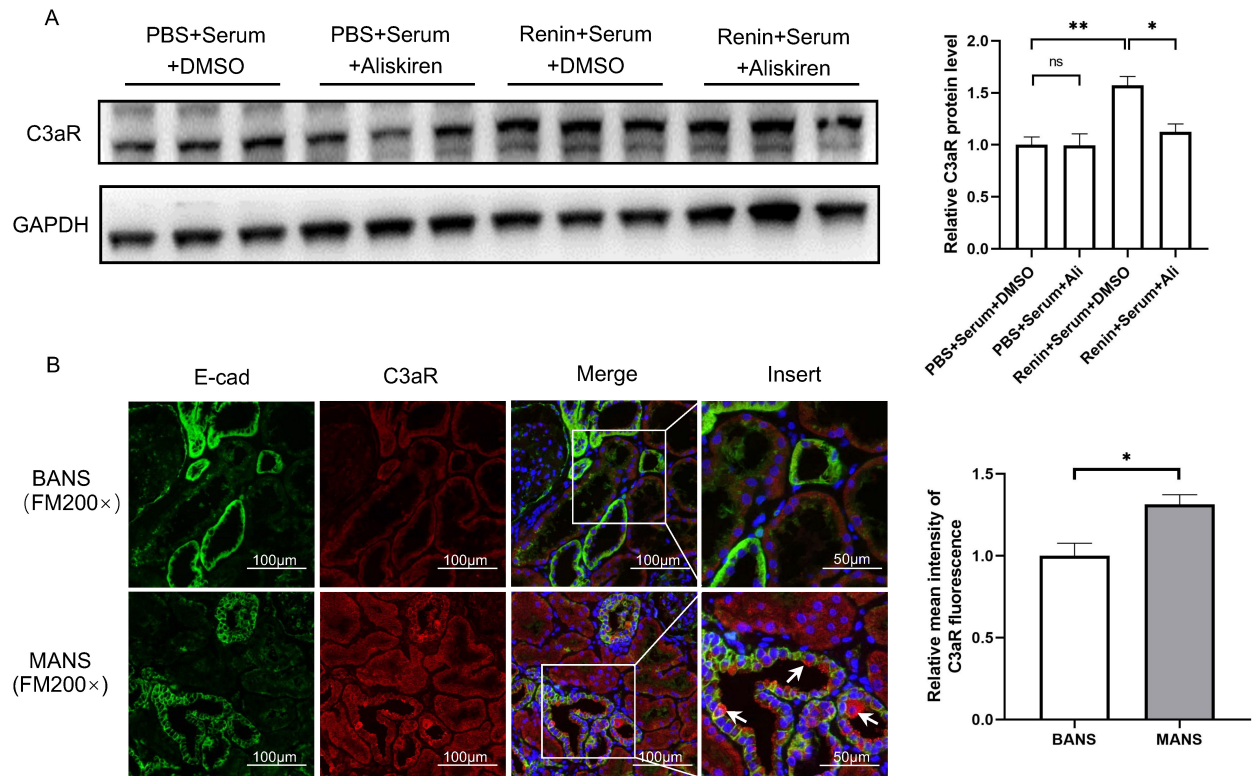


**Fig. 1. Renin induces C3aR expression in renal tubular epithelial cells.** (A) Representative western blotting images and summarized data showing the effect of renin-incubated serum and aliskiren intervention on C3aR protein levels in HK2 cells.  $N = 3$ , by one-way ANOVA. (B) Representative immunofluorescence staining images of C3aR and E-cad in kidney sections of recruited patients with MANS and BANS (200 $\times$ ; scale bar, 100  $\mu$ m; the right panel shows magnified images of the boxed areas in the left panel, arrow, positive staining of C3aR) and summarized relative mean intensity of C3aR fluorescence. MANS, malignant arteriolonephrosclerosis; BANS, benign arteriolonephrosclerosis;  $N = 3$ , by independent  $t$  test. <sup>ns</sup> $p > 0.05$ , \* $p < 0.05$ , \*\* $p < 0.01$ .

and 3 were diagnosed with MANS. Compared to patients with BANS, the patients with MANS were characterized by higher Scr, lower eGFR, higher renin activity and more severe tubulointerstitial fibrosis (Table 2). The results revealed areas with high C3aR expression in tubular epithelial cells (marked by E-cad) in patients with MANS (Fig. 1B). The relative fluorescence intensity of C3aR (Fig. 1B), as well as the plasma renin activity in MANS patients (with MANS  $2.49 \pm 0.62$  ng/mL vs. with BANS  $0.36 \pm 0.17$  ng/mL,  $t = 5.716$ ,  $p = 0.005$ ), was markedly higher than that in patients with BANS (Table 2). Pearson analysis re-

vealed that the relative fluorescence intensity of C3aR was positively correlated with renin activity levels in these patients ( $r = 0.859$ ,  $p = 0.029$ , data not shown). These results indicated that human renin could activate C3a/C3aR signaling in human tubular epithelial cells during the progression of hypertension.

### 3.3 SB290157 Restores PPAR $\alpha$ /CPT-1 $\alpha$ -Mediated Mito FAO in HK2 Cells by Inhibiting C3a/C3aR Signaling

Although renin can cleave serum C3 into C3a, it can also catalyze angiotensinogen to generate angiotensin II,

**Table 2. The characteristics and laboratory results of 6 recruited patients that accepted renal biopsy.**

Patients	Age (year)	Sex	Diagnosis	Disease duration	SBP (mmHg)	DBP (mmHg)	Scr (umol/L)	Proteinuria (mg/24 h)	eGFR (mL/min/1.73 m <sup>2</sup> )	Renin activity (ng/mL/h)	Plasma C3 (g/L)	TIF degree
P1	33	M	BANS	3 y	145	96	95	256	95.2	0.42	0.93	+
P2	65	M	BANS	30 y	143	79	140	1755	46.9	0.50	1.15	+
P3	29	M	BANS	2 m	200	110	117	7004	67.9	0.17	1.23	++
P4	29	M	MANS	2 w	220	145	259	1145	27.6	2.53	0.73	+++
P5	30	M	MANS	2 w	185	137	486	831	12.8	3.09	1.40	+++
P6	32	M	MANS	3 y	220	120	387	1623	16.6	1.85	0.83	++~+++

on BANS

M, male; SBP, systolic blood pressure; DBP, diastolic blood pressure; Scr, serum creatinine; eGFR, estimated glomerular filtration rate; MANS, malignant arteriolonephrosclerosis; BANS, benign arteriolonephrosclerosis; TIF, tubulointerstitial fibrosis degree; +, mild TIF; ++, moderate TIF; +++, severe TIF.

which also influences the downstream signaling of C3aR [30]. To avoid the effect of angiotensin II, we used a C3a analogue that has been reported in previous studies in the following experiments.

The C3a analogue also significantly increased the C3aR protein level in HK2 cells (Fig. 2A). Notably, the C3a analogue triggered the synthesis of TGF $\beta$ , a classic profibrotic factor, and promoted its secretion (Fig. 2A,B). The C3a analogue reduced the protein levels of PPAR $\alpha$ , the key regulator of Mito FAO, as well as that of CPT-1 $\alpha$ , the rate-limiting enzyme of Mito FAO in HK2 cells (Fig. 2C). Immunocytochemistry staining results also revealed decreased PPAR $\alpha$  expression in HK2 cells upon treatment with the C3a analogue (Fig. 2D). Additionally, the colocalization between the fatty acid probe and Mito tracker was decreased in HK2 cells treated with the C3a analogue, indicating a reduction in the mitochondrial uptake of fatty acids for FAO (Fig. 2E). Pretreatment of HK2 cells with the C3aR antagonist SB290157 blocked the effect induced by the C3a analogue, as indicated by a decrease in C3aR and TGF $\beta$  protein levels, an increase in PPAR $\alpha$  and CPT-1 $\alpha$  protein levels and an increase in mitochondrial uptake of fatty acids (Fig. 2). These results suggested that the activation of C3a/C3aR signaling could inhibit PPAR $\alpha$ /CPT-1 $\alpha$ -mediated tubular Mito FAO and induce TECs transformation into a profibrotic phenotype, whereas SB290157 attenuated tubular changes by targeting C3aR.

### 3.4 Rat C3 Cleavage by Renin

Renin is a species-specific enzyme. No evidence has shown whether rat renin can cleave C3 in rats. Before performing the validation experiments *in vivo*, we carried out western blotting analysis to detect the effect of rat renin on rat C3. Interestingly, western blotting analysis showed that the level of C3 cleavage increased as the concentration of renin increased, as indicated by the increasing contents of iC3b and C3c, two C3 cleavage fragments (Fig. 3A). Slight increases in the contents of iC3b and C3c were detected when purified rat C3 protein was incubated with rat recombinant renin at 1.2  $\mu$ g/mL and 12.5  $\mu$ g/mL, but not statis-

tically significant. Statistical analysis showed that renin-mediated C3 cleavage reached its highest level with 25  $\mu$ g/mL renin (Fig. 3B,C). The above results demonstrated that rat renin could cleave C3.

### 3.5 Renin Levels Increase Synchronously with C3a and C3aR Levels in the Clipped Kidneys of 2K1C Rats

Renin-dependent hypertension 2K1C rat model was used for *in vivo* experiments. As shown in Fig. 4A, the blood pressure (BP) of 2K1C rats was significantly elevated at 2 weeks ( $170 \pm 7/112 \pm 9$  mmHg) and progressed to  $205 \pm 15/137 \pm 14$  mmHg at 4 weeks after the surgery, while the BP of the sham group remained at approximately 120/50 mmHg during this period. No difference in Scr levels was found in 2K1C rats at 2 weeks compared to that of the sham group; however, at 4 weeks, the Scr levels in 2K1C rats significantly increased compared with those in sham group (Fig. 4B). Based on its higher BP and Scr levels, 4 weeks was chosen as the time point for the following experiments.

As shown in Fig. 4C, the plasma renin concentration of 2K1C rats increased markedly at 4 weeks (2K1C  $18.00 \pm 5.18$  ng/mL vs. sham  $9.61 \pm 2.06$  ng/mL,  $p < 0.05$ ). However, no difference in plasma C3a levels was found between the two groups (Fig. 4D, 2K1C  $336.6 \pm 55.3$  ng/mL vs. sham  $339.9 \pm 101.5$  ng/mL,  $p > 0.05$ ). RT-qPCR results showed a marked increase in renin mRNA levels in the clipped kidney tissues but not the nonclipped side of 2K1C rats (Fig. 4E). ELISA experiments also showed a significant increase in C3a levels in clipped kidney tissues but not in nonclipped kidney tissues (Fig. 4F). H&E staining showed that the clipped kidneys of 2K1C rats exhibited extensive tubulointerstitial injury compared with those of the rats in the sham group, with more tubular atrophy and dilation, more cast formation, more extensive inflammatory cell infiltration and higher tubular damage score (Fig. 4G,H). Masson's trichrome staining showed that the clipped kidneys of 2K1C rats manifested more collagen deposition and fibrosis foci, as evaluated by collagen volume fraction analysis (Fig. 4I,J).

After 4 weeks of 2K1C, the protein levels of C3aR and  $\alpha$ -SMA (a marker of myofibroblasts) were markedly

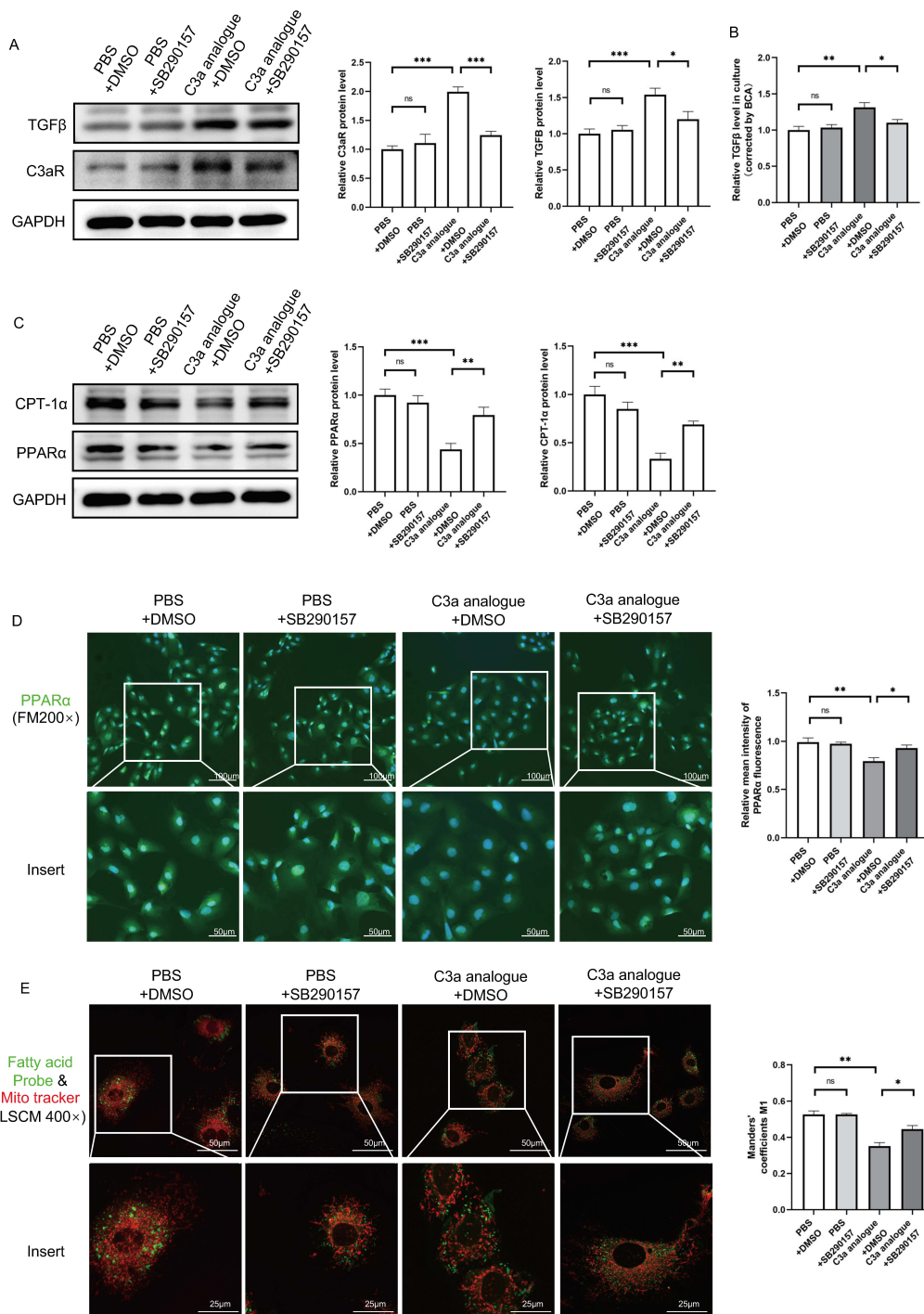


**Fig. 2. The C3aR antagonist SB290157 mitigates the C3a analogue-induced profibrotic phenotype transition and Mito FAO inhibition in HK2 cells.** (A) Representative western blotting images and summarized data of C3aR and TGFβ protein levels in HK2 cells treated with PBS, DMSO, SB290157 (1 μM, 1 h) and C3a analogue (1 μg/mL, 24 h) according to the group. (B) Summarized data of relative TGFβ levels (corrected by BCA) in the medium of HK2 cells treated with PBS, DMSO, SB290157 (1 μM, 1 h) and C3a analogue (1 μg/mL, 24 h) according to the group. N = 6. (C) Representative western blotting images, summarized data of PPARα and CPT-1α protein levels of HK2 cells treated with PBS, DMSO, SB290157 (1 μM, 1 h) and C3a analogue (1 μg/mL, 24 h) according to the group. N = 6. (D) Representative immunofluorescence staining images of PPARα (200×, scale bar, 100 μm) and summarized data of relative mean intensity of PPARα fluorescence in HK2 cells treated with PBS, DMSO, SB290157 (1 μM, 1 h) and C3a analogue (1 μg/mL, 24 h) according to the group. N = 6. (E) Representative images of the fatty acid probe and Mito tracker (400×, scale bar, 50 μm) and summarized data of Mander's coefficients in HK2 cells treated with PBS, DMSO, SB290157 (1 μM, 1 h) and C3a analogue (1 μg/mL, 24 h) according to the group. N = 3. <sup>ns</sup>*p* > 0.05, \**p* < 0.05, \*\**p* < 0.01, \*\*\**p* < 0.001 by one-way ANOVA.

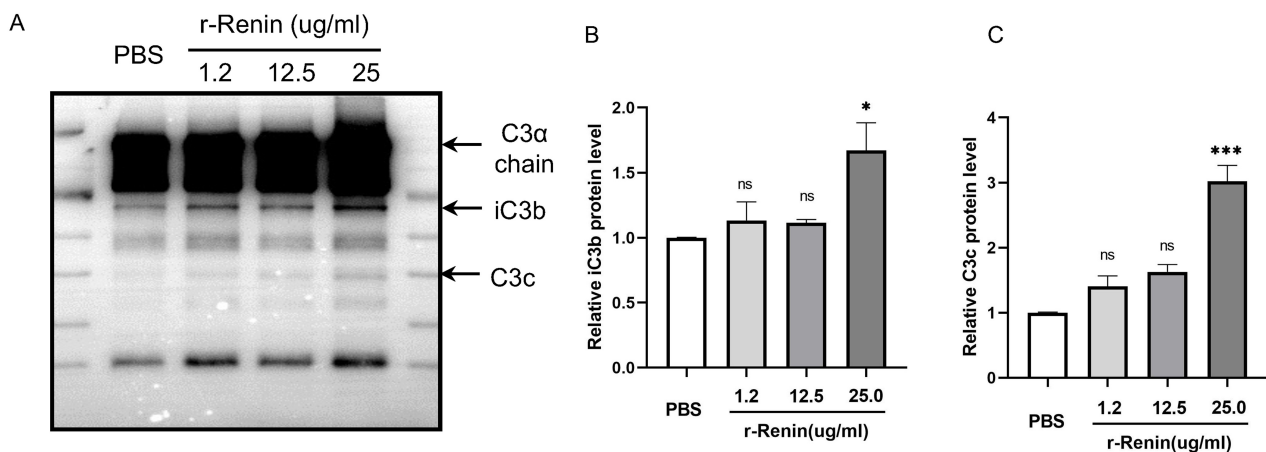


**Fig. 3. Coincubation with recombinant rat renin increases the cleavage fragments of C3.** (A) Representative western blotting images, summarized data of (B) iC3b and (C) C3c protein levels showing C3 cleavage after incubation with recombinant rat renin at 0, 1.2, 12.5 or 25  $\mu\text{g}/\text{mL}$ . r-Renin, recombinant rat renin.  $N = 3$ , <sup>ns</sup> $p > 0.05$ , \* $p < 0.05$ , \*\*\* $p < 0.001$ , vs. PBS, by one-way ANOVA.

upregulated in the clipped kidneys of 2K1C rats (Fig. 5A). RT-qPCR results also showed an increase in the mRNA levels of C3aR,  $\alpha$ -SMA, TGF $\beta$  and macrophage marker CD68 (Fig. 5B). These results suggested that C3a/C3aR signaling was activated in the clipped kidneys of rats with renovascular hypertension.

### 3.6 C3aR Inhibition Restores PPAR $\alpha$ /CPT-1 $\alpha$ -Mediated Tubular Mito FAO to Attenuate Tubulointerstitial Fibrosis in the Clipped Kidneys of 2K1C Rats

Treatment with the C3aR antagonist SB290157 did not influence the BP of 2K1C rats at 4 weeks after surgery (Fig. 6A). The renin mRNA or C3a level in the clipped kidneys of 2K1C rats was also not influenced by SB290157 (Fig. 6B,C). Of note, tubular injury and interstitial fibrosis in the clipped kidneys of 2K1C rats were attenuated by SB290157 treatment, as indicated by reduced Scr, decreased tubular damage scores and reduced collagen deposition (Fig. 6D–H). The protein levels of C3aR, TGF $\beta$  and  $\alpha$ -SMA were obviously increased in the clipped kidneys of 2K1C rats, while the treatment with SB290157 reduced these protein levels (Fig. 7A,B). Similar to the protein changes, the mRNA levels of C3aR,  $\alpha$ -SMA and TGF $\beta$  were also decreased in SB290157-treated 2K1C rats compared to vehicle-treated 2K1C rats (Fig. 7C). The increased colocalization of  $\alpha$ -SMA with CD68 in the clipped kidney cortex of 2K1C rats was mitigated by SB290157 treatment (Fig. 7D). These results revealed the ability of SB290157 to inhibit renovascular hypertension-induced tubulointerstitial fibrosis by blocking C3a/C3aR signaling.

Under TEM, a higher abundance of lipid droplets was found in the proximal TECs of the clipped kidneys of 2K1C rats. Treatment with SB290157 reduced the accumulation of lipid droplets in the proximal TECs in 2K1C rats (Fig. 8A). The protein levels of PPAR $\alpha$  and CPT-1 $\alpha$  were decreased significantly in the clipped kidneys of 2K1C rats (Fig. 8B). Accordingly, a noticeable decrease in the colocal-

ization of PPAR $\alpha$  with nuclei in TECs (marked by AQP1) was observed in the clipped kidneys of 2K1C rats (Fig. 8C). These changes were significantly alleviated by SB290157 treatment, as indicated by the restoration of PPAR $\alpha$  and CPT-1 $\alpha$  protein levels and the increased nuclear localization of PPAR $\alpha$  (Fig. 8).

## 4. Discussion

In the clinic, renin-induced hypertension combined with tubule injury remains a problem with a high prevalence. Here, we provide new *in vivo* and *in vitro* evidence that targeting C3a/C3aR signaling may achieve some benefits in the treatment of renin-dependent hypertension-induced kidney injury. In the present study, we verified that renin cleaved C3 into C3a and activated C3a/C3aR signaling in TECs. The activation of C3a/C3aR signaling played a vital role in the tubular profibrotic phenotype transition by downregulating PPAR $\alpha$ /CPT-1 $\alpha$ -mediated Mito FAO. Further results proved that the C3aR antagonist SB290157 alleviated renin-dependent hypertension-induced tubulointerstitial fibrosis by restoring PPAR $\alpha$ /CPT-1 $\alpha$ -mediated Mito FAO and inhibiting tubular profibrotic phenotypic changes.

Few previous studies have focused on the relationship of renin with C3. Only one study has reported that human renin can cleave C3 *in vitro* [6]. They also reported that murine renin was unable to act on murine C3. Renin is a species-specific enzyme. In the present study, we tested the ability of renin to cleave C3 in humans and rats. Our finding that human renin could catalyze C3 cleavage in human serum is in agreement with previously reported results [6]. Notably, our results proved that recombinant rat renin could directly cleave purified rat C3. In addition, we observed that C3a levels increased synchronically with renin in the kidney cortex of clipped kidneys in 2K1C rats. Therefore, there may exist different mechanisms of renin in mice and rats. By analyzing our data and the data reported before, we

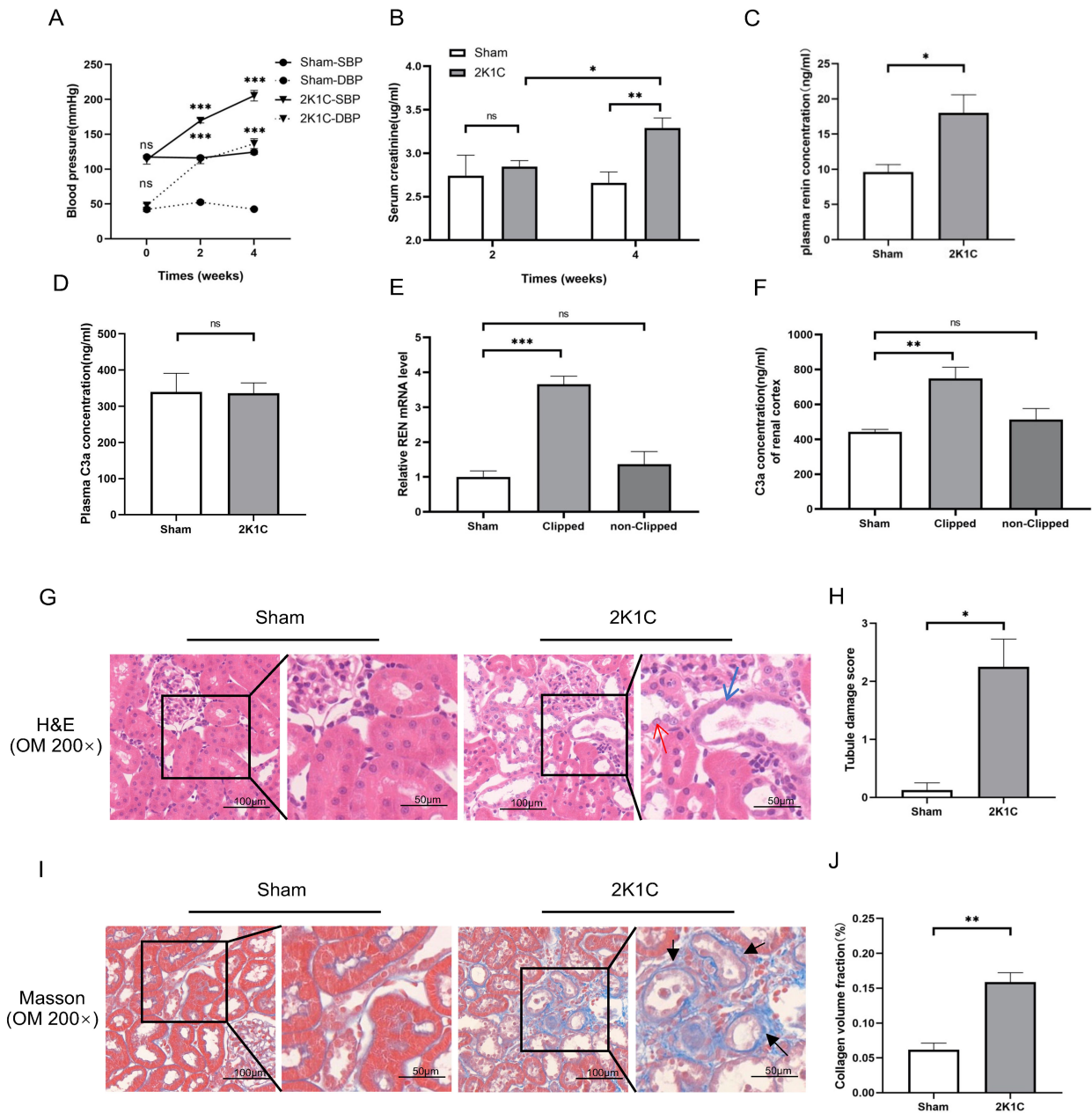


**Fig. 4. Tubulointerstitial injury, renin mRNA and C3a concentration in the clipped kidney cortex of 2K1C rats.** (A) Summarized data of blood pressure, (B) Scr levels, (C) plasma renin concentration and (D) plasma C3a concentration in sham rats and 2K1C rats. (E) Summarized data of relative REN mRNA expression and (F) C3a concentration in the renal cortex in sham rats and 2K1C rats. N = 4 per group, by one-way ANOVA. (G) Representative H&E staining images, (H) summarized data of tubular damage scores, (I) representative Masson staining images and (J) summarized data of collagen volume fraction of the kidney cortex in sham rats and 2K1C rats (clipped kidney) (200 $\times$ ; scale bar, 100  $\mu$ m; the right panel shows magnified images of the boxed areas in the left panel; blue arrow, atrophic tubule; red arrow, injured tubule; black arrow, fibrosis foci). SBP, systolic blood pressure; DBP, diastolic blood pressure; Scr, serum creatinine; N = 4 per group, by independent *t* test. <sup>ns</sup>*p* > 0.05, \**p* < 0.05, \*\**p* < 0.01, \*\*\**p* < 0.001.

find that 1.2  $\mu$ g/mL recombinant human renin could achieve significant C3 cleavage while in rat 25  $\mu$ g/mL recombinant renin was required, suggesting a weaker C3 cleavage effect of rat renin.

In different disease models, the location of the C3aR protein in the kidney cortex has been reported to differ from that under normal conditions. Under normal conditions,

C3aR distribution is restricted to renal epithelial cells and interstitial cells [16,17]. However, high C3aR expression in podocytes, mesangial cells and endothelial cells has been reported in patients and animals with various chronic kidney diseases [19,31,32]. Here, we showed increased C3aR expression in the TECs of MANS patients with high renin activity. In comparison, C3aR expression in the TECs of

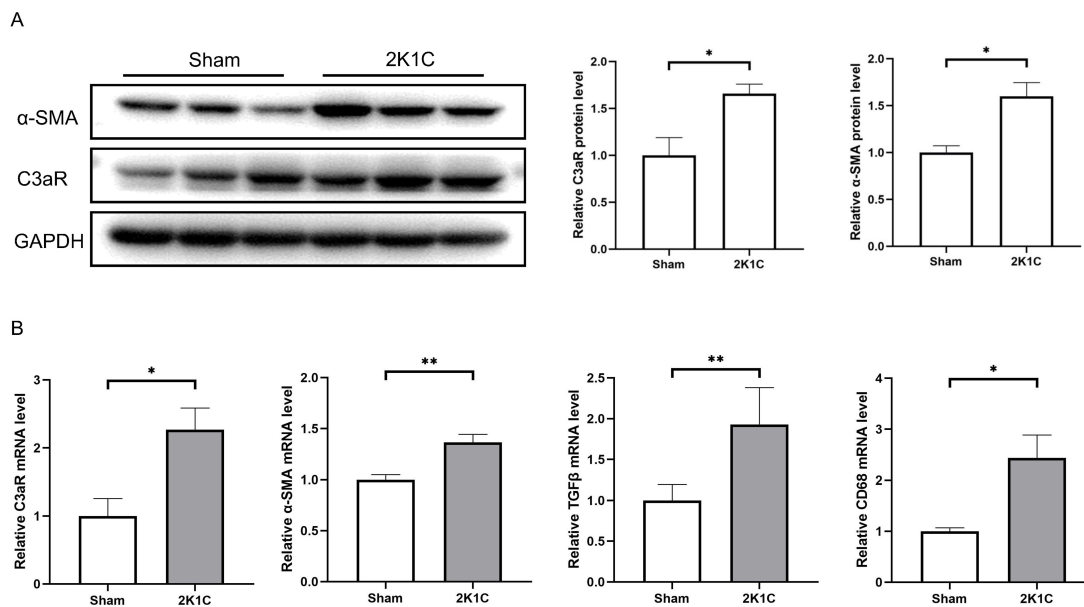


**Fig. 5. C3aR and mesenchymal transition markers increase in the kidney cortex of 2K1C rats.** (A) Representative western blotting images, summarized data of C3aR and  $\alpha$ -SMA protein levels and (B) summarized C3aR,  $\alpha$ -SMA, TGF $\beta$  and CD68 mRNA levels in the renal cortex in sham rats and 2K1C rats (clipped kidney). N = 4 per group. \* $p < 0.05$ , \*\* $p < 0.01$  by independent  $t$  test.

BANS patients was much lower. These results are in line with a previous report that more complement components, including C3a, were found in MANS patients than in BANS patients and normal controls [12]. Our results provide a novel mechanism of the RAS in renal injury by activating C3a/C3aR signaling, especially in malignant hypertensive patients with a high renin state.

The location of sites with high C3aR expression indicates the potential involvement of C3a/C3aR signaling in renin-dependent hypertension-induced tubulointerstitial fibrosis. It is known that TECs adopt a profibrotic phenotype and secrete profibrotic factors, including TGF $\beta$  in the chronic kidney injury environment [33–35]. In our study, we detected an increase in TGF $\beta$  expression in HK2 cells, as well as an increase in TGF $\beta$  concentration in the culture medium, after C3a/C3aR activation. In addition, we found a significant decrease in PPAR $\alpha$ -CPT1 $\alpha$ -mediated tubular Mito FAO, which has been reported to occur along with TGF $\beta$ -mediated tubular interstitial fibrosis. Another study also demonstrated that defective FAO can promote TECs to secrete TGF $\beta$  and tubular profibrotic phenotype transition [36]. In addition, PPAR $\alpha$  agonists have been reported to help reduce TGF $\beta$  expression and downstream signaling to mitigate hypertension-induced kidney injury in spontaneous hypertensive rats [37]. As the most important profibrotic cytokine, TGF $\beta$  plays a fundamental role in myofibroblast transition [38], which serves as the main mechanism of tubulointerstitial fibrosis. Infiltrating monocyte-derived macrophages are one of the important sources of myofibroblasts in the kidney interstitium [39]. The macrophage-to-myofibroblast transition can be mediated by TGF $\beta$  by canonical smad2/3 signal-

ing and other noncanonical signaling pathways [40,41]. In the current study, similar mesenchymal transition mechanisms were observed in renin-dependent hypertension-induced kidney injury and were closely associated with renin-induced C3a/C3aR activation in TECs. Our results provide new evidence that renin-induced C3a/C3aR signaling participates in hypertension-induced tubulointerstitial fibrosis by facilitating mesenchymal transition. Taken together, these results show that C3a/C3aR activation plays a vital role in accelerating hypertension-induced kidney injury.

Another important finding in our study is that renin/C3a/C3aR activation impairs PPAR $\alpha$ /CPT1 $\alpha$ -mediated tubular Mito FAO in rats suffering from hypertension. C3a/C3aR signaling has emerged as a critical regulator of cellular metabolism in recent years. One study showed that the activation of C3a/C3aR altered the metabolic phenotype of synovial fibroblasts from mitochondrial respiration to aerobic glycolysis [42]. However, no study has elucidated the detailed mechanisms how C3a/C3aR influences the downstream factor PPAR $\alpha$  in TECs, and there are clues suggesting the potential of C3aR in regulating PPAR $\alpha$ -mediated Mito FAO. Studies have reported that C3a/C3aR activation inhibited cAMP-PKA signaling by activating G $\alpha$ i [43] to modulate mitochondrial function and energy restoration in different tissue cells [44,45]. Other studies have provided evidence that cAMP-PKA signaling plays an important role in activating PPAR $\alpha$  [46,47]. Therefore, we speculate that cAMP-PKA signaling inhibition by C3a/C3aR may cause impaired PPAR $\alpha$ -mediated Mito FAO in TECs. However, the detailed mechanisms still need to be further investigated.

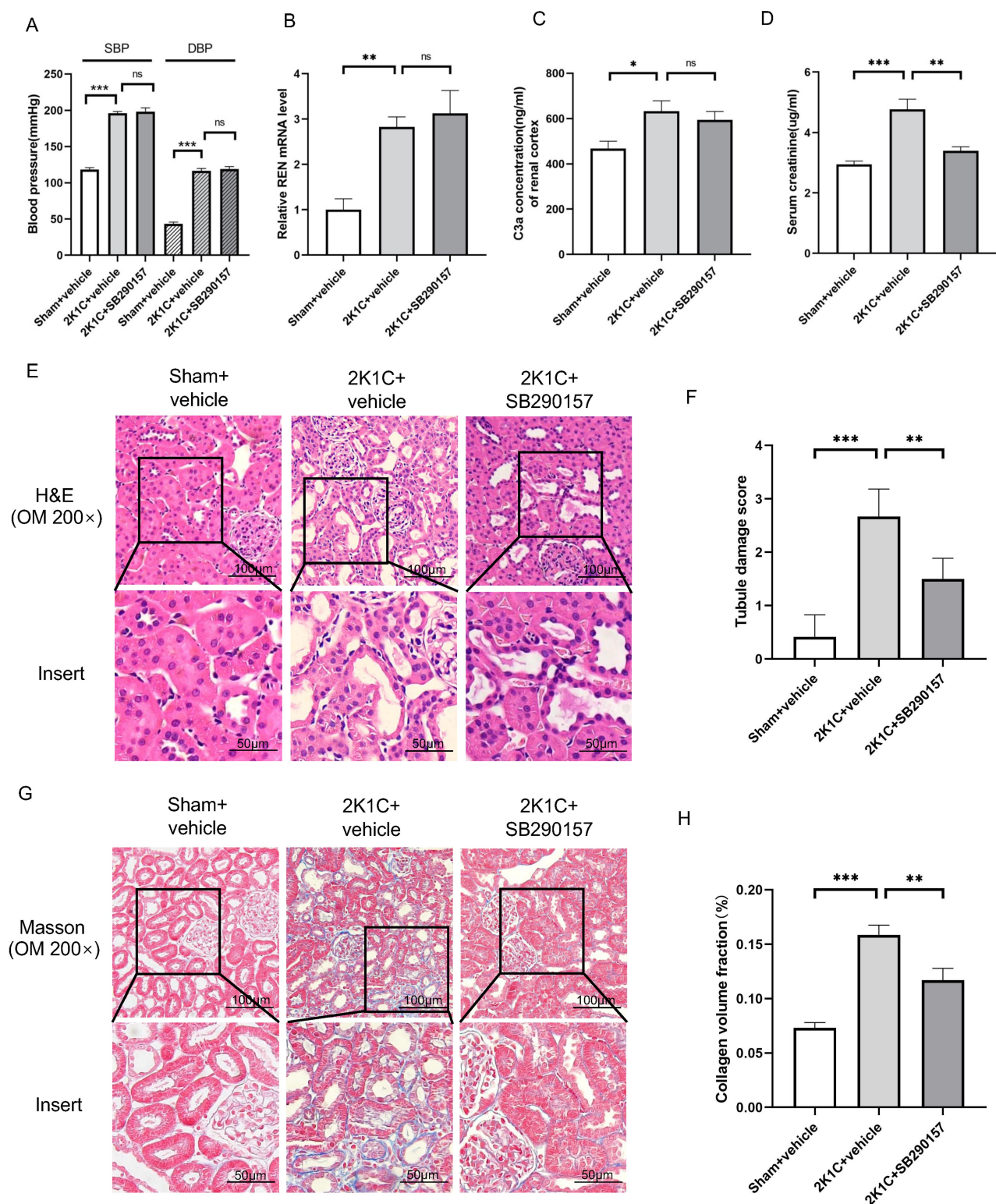


**Fig. 6. The C3aR antagonist SB290157 alleviates tubulointerstitial fibrosis in 2K1C rats.** (A) Summarized blood pressure and (D) Scr levels in sham+vehicle, 2K1C+vehicle and 2K1C+ SB290157 rats. N = 6 per group. (B) Summarized REN mRNA levels and (C) C3a concentration in the renal cortex in sham+vehicle, 2K1C+vehicle (clipped kidney) and 2K1C+SB290157 (clipped kidney) rats. N = 6 per group. (E) Representative H&E staining images, (F) summarized tubular damage scores, (G) representative Masson staining images and (H) summarized collagen volume fraction of the renal cortex in sham+vehicle, 2K1C+vehicle (clipped kidney) and 2K1C+SB290157 (clipped kidney) rats (200 $\times$ ; scale bar, 100  $\mu$ m; the lower panel shows magnified images of the boxed areas in the upper panel). N = 6 per group. <sup>ns</sup> $p > 0.05$ ,  $*p < 0.05$ ,  $**p < 0.01$ ,  $***p < 0.001$  by one-way ANOVA.

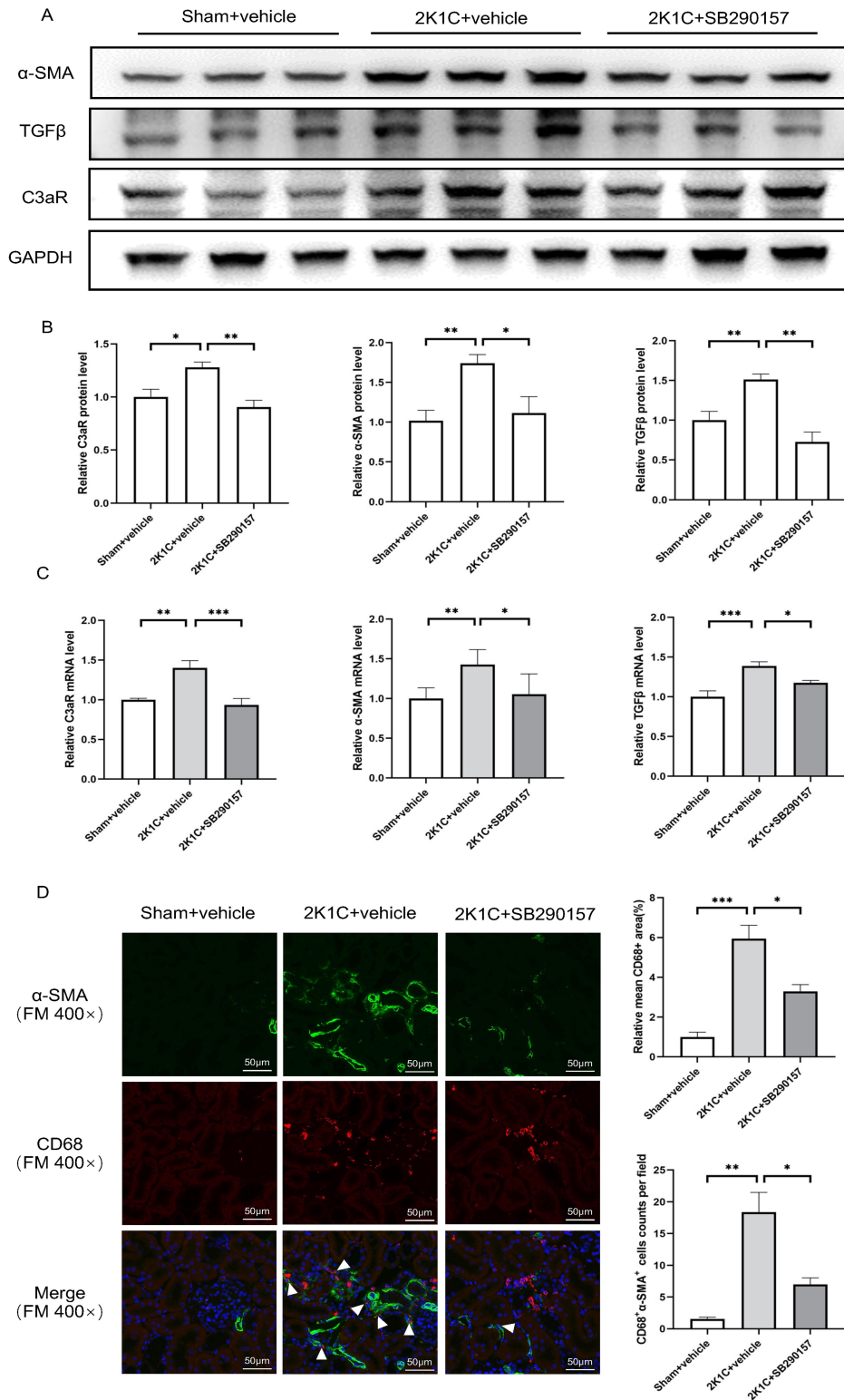


**Fig. 7. The C3aR antagonist SB290157 reduces C3aR expression and mesenchymal transition in 2K1C rats.** (A) Representative western blotting images and (B) summarized data of C3aR,  $\alpha$ -SMA and TGF $\beta$  protein and (C) mRNA levels of the renal cortex in sham+vehicle, 2K1C+vehicle (clipped kidney) and 2K1C+SB290157 (clipped kidney) rats. N = 6 per group. (D) Representative immunofluorescence staining images of  $\alpha$ -SMA and CD68 (400 $\times$ ; scale bar, 50  $\mu$ m; white triangles, colocalization of  $\alpha$ -SMA and CD68) and summarized data of relative CD68-positive area (%) and CD68<sup>+</sup> $\alpha$ -SMA<sup>+</sup> cell counts per field in the renal cortex of sham+vehicle, 2K1C+vehicle (clipped kidney) and 2K1C+SB290157 (clipped kidney) rats. N = 3 per group, \* $p$  < 0.05, \*\* $p$  < 0.01, \*\*\* $p$  < 0.001 by one-way ANOVA.

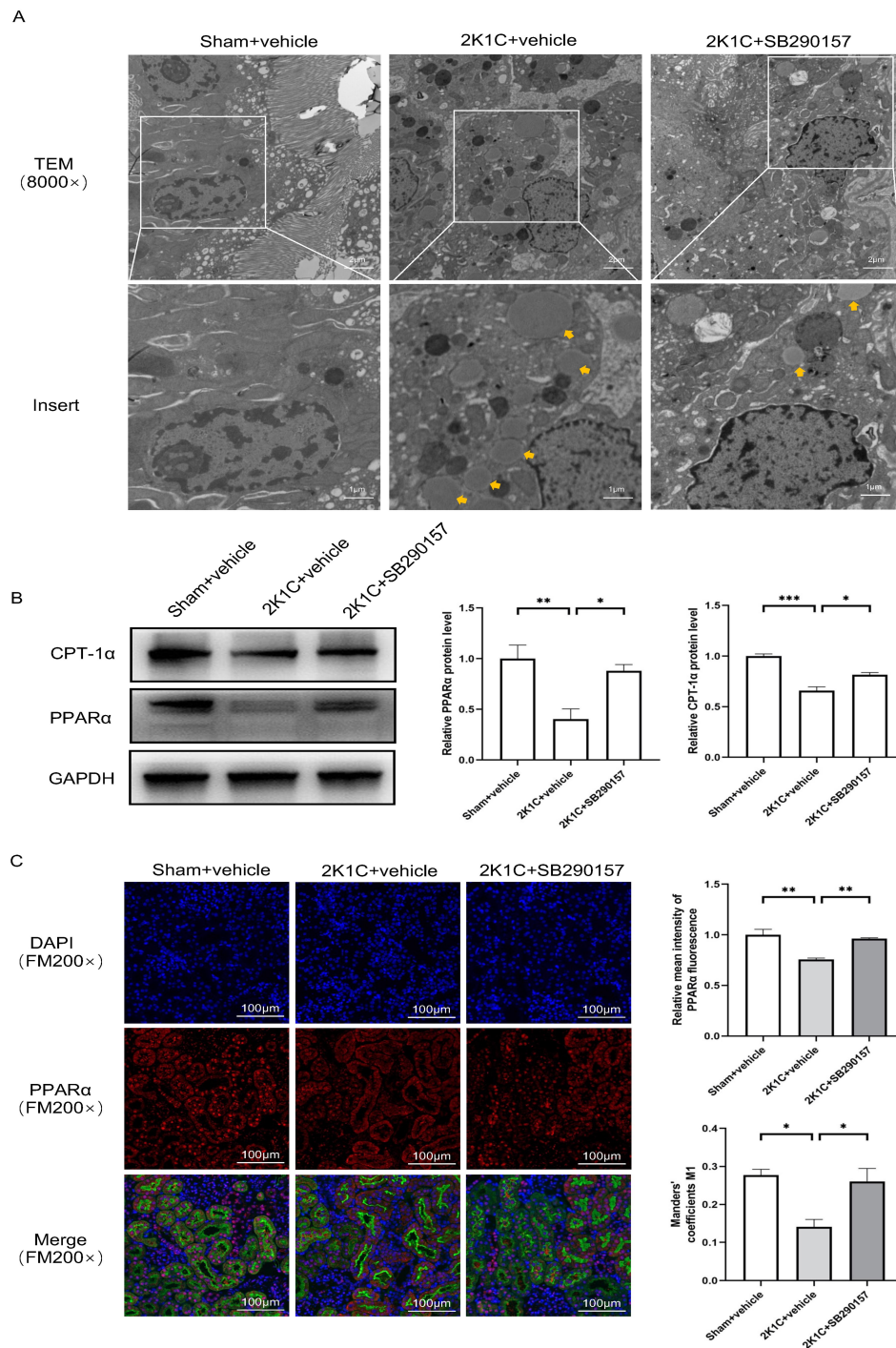


**Fig. 8. The C3aR antagonist SB290157 restores PPAR $\alpha$ /CPT-1 $\alpha$ -mediated tubular Mito FAO.** (A) Representative TEM images of proximal TECs (8000 $\times$ ; scale bar, 2  $\mu$ m; the lower panel shows magnified images of the boxed areas in the upper panel; yellow arrows, lipid droplet) in the renal cortex of sham+vehicle, 2K1C+vehicle (clipped kidney) and 2K1C+SB290157 (clipped kidney) rats. N = 3 per group. (B) Representative western blotting images and summarized PPAR $\alpha$  and CPT-1 $\alpha$  protein levels in the renal cortex of sham+vehicle, 2K1C+vehicle (clipped kidney) and 2K1C+SB290157 (clipped kidney) rats. N = 6 per group. (C) Representative immunofluorescence staining images of PPAR $\alpha$  and DAPI (200 $\times$ ; scale bar, 100  $\mu$ m; TECs marked by AQP1 with green fluorescence), summarized data of relative mean intensity of PPAR $\alpha$  fluorescence and Manders' coefficients of PPAR $\alpha$  and DAPI in the renal cortex of sham+vehicle, 2K1C+vehicle (clipped kidney) and 2K1C+SB290157 (clipped kidney) rats. N = 3 per group. \* $p$  < 0.05, \*\* $p$  < 0.01, \*\*\* $p$  < 0.001 by one-way ANOVA.

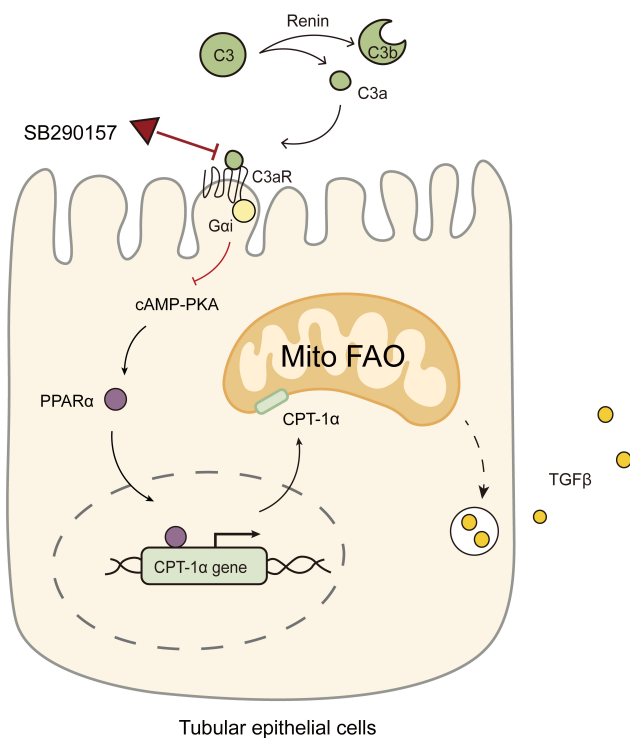


**Fig. 9. Diagram showing the C3aR antagonist SB290157 targeting C3a/C3aR signaling to restore PPAR $\alpha$ /CPT-1 $\alpha$ -mediated MitoFAO and offset tubular profibrotic phenotype transition in renin-dependent hypertension-induced kidney injury.**

C3a/C3aR signaling is widely involved in kidney diseases through various mechanisms [48]. In acute kidney injury, there is controversy about the role of C3a/C3aR signaling. Reportedly, C3a promotes the synthesis of inflammatory mediators and chemokines in ischemia–reperfusion induced kidney injury [49,50]. In Shiga toxin-associated hemolytic uremic syndrome, C3a/C3aR signaling activation induces mitochondrial dysfunction and imbalances the redox state to aggravate tubular injury [51]. However, C3a/C3aR activation in sepsis-induced kidney injury has been demonstrated to be a protective way to limit the bacterial load and renal damage [27]. In most CKD models, C3a/C3aR signaling is defined as dangerous signaling that stimulates the synthesis of proinflammatory and profibrotic cytokines in renal paranchymal cells and infiltrating cells [52,53]. In addition, C3a is reported to be an important inducer of the cellular mesenchymal transition, including that of epithelial cells and endothelial cells [19,32]. Our study verifies the effect of C3a/C3aR activation in promoting tubulointerstitial fibrosis in hypertension-induced CKD. Inhibiting C3a/C3aR signaling is likely to be a potential therapeutic strategy in hypertensive subjects with tubulointerstitial fibrosis.

The C3aR antagonist SB290157 has been confirmed as a C3aR inhibitor in the lung [22], brain [54], heart [55] and kidney [31,44,56]. SB290157 treatment has proven

beneficial in chronic renal fibrosis. Given the curative potential of SB290157, we performed a series of experiments to test its effect on renin-dependent hypertension-induced kidney injury. Our data are the first to demonstrate that SB290157 significantly mitigates renin-dependent hypertension-induced Mito FAO defects and tubular profibrotic phenotype transition by blocking C3a/C3aR signaling. In clinical practice, ACEIs and ARBs are frequently used to treat hypertension patients with RAS activation. However, the utilization of these drugs results in persistent renin elevation. Therefore, the blockage of C3aR may be a potent strategy for preventing tubulointerstitial injury. Of note, the inhibitor of another anaphylatoxin receptor, the C5aR inhibitor avacopan, has been approved by the FDA to treat anti-neutrophil cytoplasmic antibody (ANCA)-associated vasculitis [57]. No C3aR inhibitor is currently available in the clinic. We believe that C3aR inhibitors may be a potential treatment for renin-dependent hypertension-induced kidney injury in the future.

## 5. Limitations

There are a few limitations of the current study. First, our study is limited by the small sample size of patients and rats employed. And we did not directly detect the C3a protein in western blotting analysis because of the lack of a C3a-specific antibody. The levels of C3a measured in tissue homogenate may underestimate the C3a concentration in clipped kidneys due to the limitations of an ELISA from tissue homogenate, as a portion of C3a may remain within the tissue matrix. We did not use the renin inhibitor aliskiren to treat 2K1C rats since its ability to inhibit renin activity in rodents has been reported to be weak [58].

Another potential limitation of our study is that we did not verify the specificity of SB290157 due to its agonistic effect on C5aR2 [59]. To prove the effect of SB290157 on C3aR, an *in vitro* calcium assay would be a possibility considering that SB290157 could inhibit the influx of Ca<sup>2+</sup> which is increased by C3a stimulation [60,61]. But the therapeutic effect of SB290157 *in vivo* is hard to confirm. Despite the off-target effect of SB290157 on C5aR2, we believe that it has limited effect on our current results on account that a weak C5aR2 expression in TECs [62,63] and an insignificant effect of C5aR2 in either acute kidney injury or chronic renal fibrosis models has been reported previously [64,65].

At last, we only evaluated the role of SB290157 in 2K1C rat model to simulate renin-dependent hypertension status *in vivo*. For the translation of our findings to clinical applications, it is necessary to further confirm the effect of SB290157 in additional models of renin-dependent hypertension, for instance, spontaneous hypertension rats and double transgenic rats harboring both the human renin and human angiotensinogen genes (dTGR), in future studies.

## 6. Conclusions

The results of our study provide strong evidence that renin can cleave C3 into C3a and activate C3a/C3aR signaling in TECs to impair PPAR $\alpha$ /CPT-1 $\alpha$ -mediated Mito FAO both *in vivo* and *in vitro*. Treatment with SB290157 significantly mitigates renin-dependent hypertension-induced tubular profibrotic phenotype transition by blocking C3a/C3aR signaling. In summary, although in-depth studies and pilot trials are still warranted, our findings suggest that SB290157 treatment attenuates renin-dependent hypertension-induced tubulointerstitial fibrosis by restoring PPAR $\alpha$ /CPT-1 $\alpha$ -mediated Mito FAO and reversing the phenotypic transition of TECs through C3a/C3aR signaling (Fig. 9).

## Abbreviations

ANCA, anti-neutrophil cytoplasmic antibody; AQP1, aquaporin 1; BANS, benign arteriolar nephrosclerosis; BCA, bicinchoninic acid assay; BP, blood pressure; CKD, chronic kidney diseases; CPT-1 $\alpha$ , carnitine palmitoyltransferase-1 $\alpha$ ; C3aR, C3a receptor; DMEM/F12, dulbecco's modified eagle's medium/nutrient mixture F-12; DPBS, dulbecco's phosphate buffered saline; E-cad, e-cadherin; FBS, fetal bovine serum; HK2, human kidney 2 cells; H&E, hematoxylin-eosin; MANS, malignant arteriolar nephrosclerosis; PBS, phosphate buffered saline; PPAR $\alpha$ , peroxisome proliferator-activated receptor alpha; PVDF, polyvinylidene difluoride; RT-qPCR, real time-quantitative polymerase chain reaction; Scr, serum creatinine; SDS-PAGE, sodium dodecyl sulphate-polyacrylamide gel electrophoresis; TECs, tubular epithelial cells; TGF $\beta$ , transforming growth factor  $\beta$ ;  $\alpha$ -SMA,  $\alpha$ -smooth muscle actin; 2K1C, two-kidney one-clipped.

## Availability of Data and Materials

The datasets used and/or analyzed in the current study are available from the corresponding author on reasonable request.

## Author Contributions

CW, ZW and WZ designed the research study. CW, ZW and KJ performed the research. TX collected the clinical data. CW, ZW and HM analyzed the data. JX and XP provided help on the analysis of histological images and transmission electron microscopy images. XF made contributions to data interpretation. XF and WZ provided supervision. CW and ZW wrote the manuscript. All authors contributed to editorial changes in the manuscript. All authors approved the final version of the paper. All authors have participated sufficiently in the work and agreed to be accountable for all aspects of the work.

## Ethics Approval and Consent to Participate

The study protocol has been approved by the Ethics Committee of Ruijin Hospital, Shanghai Jiao Tong Univer-

sity School of Medicine (approval number 20220-319). Patient information was managed according to applicable data protection regulations. All participating individuals have given their written informed consent to participate in the study. Animal study was conducted according to the guidelines of the Declaration of Helsinki, and approved by the Ethic Committee on Animal Care of Charles River Laboratories (approval number P2021100).

## Acknowledgment

We are grateful for the sacrifice of the animals in this study and thank all the participating staff of the Department of Nephrology, Ruijin Hospital, Shanghai Jiao Tong University. We thank all the patients participated in the study for their cooperation.

## Funding

This study was funded by the National Natural Science Foundation of China (Grant number 81470967, 81670613 and 82270705) and the Shanghai Science and Technology Committee (Grant number 21ZR1440300).

## Conflict of Interest

The authors declare no conflict of interest.

## References

- [1] NCD Risk Factor Collaboration (NCD-RisC). Worldwide trends in hypertension prevalence and progress in treatment and control from 1990 to 2019: a pooled analysis of 1201 population-representative studies with 104 million participants. *Lancet* (London, England). 2021; 398: 957–980.
- [2] Collaborators GBDRF. Global, regional, and national comparative risk assessment of 84 behavioural, environmental and occupational, and metabolic risks or clusters of risks for 195 countries and territories, 1990-2017: a systematic analysis for the Global Burden of Disease Study 2017. *Lancet*. 2018; 392: 1923–1994.
- [3] Jackson KL, Marques FZ, Watson AMD, Palma-Rigo K, Nguyen-Huu TP, Morris BJ, *et al.* A novel interaction between sympathetic overactivity and aberrant regulation of renin by miR-181a in BPH/2J genetically hypertensive mice. *Hypertension* (Dallas, Tex.: 1979). 2013; 62: 775–781.
- [4] Welch WJ. The pathophysiology of renin release in renovascular hypertension. *Seminars in Nephrology*. 2000; 20: 394–401.
- [5] Crowley SD, Rudemiller NP. Immunologic Effects of the Renin-Angiotensin System. *Journal of the American Society of Nephrology: JASN*. 2017; 28: 1350–1361.
- [6] Békássy ZD, Kristoffersson AC, Rebetz J, Tati R, Olin AI, Karpman D. Aliskiren inhibits renin-mediated complement activation. *Kidney International*. 2018; 94: 689–700.
- [7] Shagdarsuren E, Wellner M, Braesen JH, Park JK, Fiebeler A, Henke N, *et al.* Complement activation in angiotensin II-induced organ damage. *Circulation Research*. 2005; 97: 716–724.
- [8] Mizerska-Wasiak M, Such-Gruchot A, Cichoń-Kawa K, Turczyn A, Małyk J, Miklaszewska M, *et al.* The Role of Complement Component C3 Activation in the Clinical Presentation and Prognosis of IgA Nephropathy-A National Study in Children. *Journal of Clinical Medicine*. 2021; 10: 4405.
- [9] Bomback AS, Santoriello D, Avastare RS, Regunathan-Shenk R, Canetta PA, Ahn W, *et al.* C3 glomerulonephritis and dense deposit disease share a similar disease course in a large United

- States cohort of patients with C3 glomerulopathy. *Kidney International*. 2018; 93: 977–985.
- [10] Zhang Y, Li Z, Wu H, Wang J, Zhang S. Esculetin alleviates murine lupus nephritis by inhibiting complement activation and enhancing Nrf2 signaling pathway. *Journal of Ethnopharmacology*. 2022; 288: 115004.
  - [11] Bode M, Diemer JN, Luu TV, Ehnert N, Teigeler T, Wiech T, *et al.* Complement component C3 as a new target to lower albuminuria in hypertensive kidney disease. *British Journal of Pharmacology*. 2023. (online ahead of print)
  - [12] Timmermans SAMEG, Abdul-Hamid MA, Vanderlocht J, Damoiseaux JGMC, Reutelingsperger CP, van Paassen P, *et al.* Patients with hypertension-associated thrombotic microangiopathy may present with complement abnormalities. *Kidney International*. 2017; 91: 1420–1425.
  - [13] Zhang Y, Yang C, Zhou X, Hu R, Quan S, Zhou Y, *et al.* Association between thrombotic microangiopathy and activated alternative complement pathway in malignant nephrosclerosis. *Nephrology, Dialysis, Transplantation: Official Publication of the European Dialysis and Transplant Association - European Renal Association*. 2020; gfaa280.
  - [14] Wang W, Sheng L, Chen Y, Li Z, Wu H, Ma J, *et al.* Total coumarin derivatives from *Hydrangea paniculata* attenuate renal injuries in cationized-BSA induced membranous nephropathy by inhibiting complement activation and interleukin 10-mediated interstitial fibrosis. *Phytotherapy and Phytopharmacology*. 2022; 96: 153886.
  - [15] Sun J, Ember JA, Chao TH, Fukuoka Y, Ye RD, Hugli TE. Identification of ligand effector binding sites in transmembrane regions of the human G protein-coupled C3a receptor. *Protein Science: a Publication of the Protein Society*. 1999; 8: 2304–2311.
  - [16] Braun MC, Reins RY, Li TB, Hollmann TJ, Dutta R, Rick WA, *et al.* Renal expression of the C3a receptor and functional responses of primary human proximal tubular epithelial cells. *Journal of Immunology (Baltimore, Md.: 1950)*. 2004; 173: 4190–4196.
  - [17] Kiafard Z, Tschernig T, Schweyer S, Bley A, Neumann D, Zwirner J. Use of monoclonal antibodies to assess expression of anaphylatoxin receptors in tubular epithelial cells of human, murine and rat kidneys. *Immunobiology*. 2007; 212: 129–139.
  - [18] Zhou X, Fukuda N, Matsuda H, Endo M, Wang X, Saito K, *et al.* Complement 3 activates the renal renin-angiotensin system by induction of epithelial-to-mesenchymal transition of the nephrotubulus in mice. *American Journal of Physiology. Renal Physiology*. 2013; 305: F957–F967.
  - [19] Tang Z, Lu B, Hatch E, Sacks SH, Sheerin NS. C3a mediates epithelial-to-mesenchymal transition in proteinuric nephropathy. *Journal of the American Society of Nephrology: JASN*. 2009; 20: 593–603.
  - [20] Han R, Hu S, Qin W, Shi J, Hou Q, Wang X, *et al.* C3a and suPAR drive versican V1 expression in tubular cells of focal segmental glomerulosclerosis. *JCI Insight*. 2019; 4: e130986.
  - [21] Liu Y, Wang K, Liang X, Li Y, Zhang Y, Zhang C, *et al.* Complement C3 Produced by Macrophages Promotes Renal Fibrosis via IL-17A Secretion. *Frontiers in Immunology*. 2018; 9: 2385.
  - [22] Gu H, Fisher AJ, Mickler EA, Duerson F, 3rd, Cummings OW, Peters-Golden M, *et al.* Contribution of the anaphylatoxin receptors, C3aR and C5aR, to the pathogenesis of pulmonary fibrosis. *FASEB Journal: Official Publication of the Federation of American Societies for Experimental Biology*. 2016; 30: 2336–2350.
  - [23] Weng H, Ji X, Endo K, Iwai N. Pex11a deficiency is associated with a reduced abundance of functional peroxisomes and aggravated renal interstitial lesions. *Hypertension (Dallas, Tex.: 1979)*. 2014; 64: 1054–1060.
  - [24] Kunchithapatham K, Atkinson C, Rohrer B. Smoke exposure causes endoplasmic reticulum stress and lipid accumulation in retinal pigment epithelium through oxidative stress and complement activation. *The Journal of Biological Chemistry*. 2014; 289: 14534–14546.
  - [25] Song NJ, Kim S, Jang BH, Chang SH, Yun UJ, Park KM, *et al.* Small Molecule-Induced Complement Factor D (Adipsin) Promotes Lipid Accumulation and Adipocyte Differentiation. *PLoS ONE*. 2016; 11: e0162228.
  - [26] Wang Z, Fu Z, Wang C, Xu J, Ma H, Jiang M, *et al.* ZLN005 protects against ischemia-reperfusion-induced kidney injury by mitigating oxidative stress through the restoration of mitochondrial fatty acid oxidation. *American Journal of Translational Research*. 2021; 13: 10014–10037.
  - [27] Wu KY, Zhang T, Zhao GX, Ma N, Zhao SJ, Wang N, *et al.* The C3a/C3aR axis mediates anti-inflammatory activity and protects against uropathogenic *E. coli*-induced kidney injury in mice. *Kidney International*. 2019; 96: 612–627.
  - [28] Ember JA, Johansen NL, Hugli TE. Designing synthetic superagonists of C3a anaphylatoxin. *Biochemistry*. 1991; 30: 3603–3612.
  - [29] Jensen EC. Quantitative analysis of histological staining and fluorescence using ImageJ. *Anatomical Record (Hoboken, N.J.: 2007)*. 2013; 296: 378–381.
  - [30] Chen XH, Ruan CC, Ge Q, Ma Y, Xu JZ, Zhang ZB, *et al.* Deficiency of Complement C3a and C5a Receptors Prevents Angiotensin II-Induced Hypertension via Regulatory T Cells. *Circulation Research*. 2018; 122: 970–983.
  - [31] Gao S, Cui Z, Zhao MH. Complement C3a and C3a Receptor Activation Mediates Podocyte Injuries in the Mechanism of Primary Membranous Nephropathy. *Journal of the American Society of Nephrology: JASN*. 2022; 33: 1742–1756.
  - [32] Li L, Chen L, Zang J, Tang X, Liu Y, Zhang J, *et al.* C3a and C5a receptor antagonists ameliorate endothelial-myofibroblast transition via the Wnt/ $\beta$ -catenin signaling pathway in diabetic kidney disease. *Metabolism: Clinical and Experimental*. 2015; 64: 597–610.
  - [33] Lu YA, Liao CT, Raybould R, Talabani B, Grigorieva I, Szomolay B, *et al.* Single-Nucleus RNA Sequencing Identifies New Classes of Proximal Tubular Epithelial Cells in Kidney Fibrosis. *Journal of the American Society of Nephrology: JASN*. 2021; 32: 2501–2516.
  - [34] Chen J, Chen KH, Wang LM, Luo J, Zheng QY, He YN. Decoy receptor 2 mediates the apoptosis-resistant phenotype of senescent renal tubular cells and accelerates renal fibrosis in diabetic nephropathy. *Cell Death & Disease*. 2022; 13: 522.
  - [35] Wu CF, Chiang WC, Lai CF, Chang FC, Chen YT, Chou YH, *et al.* Transforming growth factor  $\beta$ -1 stimulates profibrotic epithelial signaling to activate pericyte-myofibroblast transition in obstructive kidney fibrosis. *The American Journal of Pathology*. 2013; 182: 118–131.
  - [36] Liu L, Liu T, Jia R, Zhang L, Lv Z, He Z, *et al.* Downregulation of fatty acid oxidation led by Hlpda increases G2/M arrest/delay-induced kidney fibrosis. *Biochimica et Biophysica Acta. Molecular Basis of Disease*. 2023; 1869: 166701.
  - [37] Hou X, Shen YH, Li C, Wang F, Zhang C, Bu P, *et al.* PPAR-alpha agonist fenofibrate protects the kidney from hypertensive injury in spontaneously hypertensive rats via inhibition of oxidative stress and MAPK activity. *Biochemical and Biophysical Research Communications*. 2010; 394: 653–659.
  - [38] Meng XM, Nikolic-Paterson DJ, Lan HY. TGF- $\beta$ : the master regulator of fibrosis. *Nature Reviews. Nephrology*. 2016; 12: 325–338.
  - [39] Nikolic-Paterson DJ, Wang S, Lan HY. Macrophages promote renal fibrosis through direct and indirect mechanisms. *Kidney International Supplements*. 2014; 4: 34–38.
  - [40] Wang S, Meng XM, Ng YY, Ma FY, Zhou S, Zhang Y, *et al.* TGF- $\beta$ /Smad3 signalling regulates the transition of bone marrow-derived macrophages into myofibroblasts during tissue fibrosis. *Oncotarget*. 2016; 7: 8809–8822.

- [41] Yang Y, Feng X, Liu X, Wang Y, Hu M, Cao Q, *et al.* Fate alteration of bone marrow-derived macrophages ameliorates kidney fibrosis in murine model of unilateral ureteral obstruction. *Nephrology, Dialysis, Transplantation: Official Publication of the European Dialysis and Transplant Association - European Renal Association.* 2019; 34: 1657–1668.
- [42] Friščić J, Böttcher M, Reinwald C, Bruns H, Wirth B, Popp SJ, *et al.* The complement system drives local inflammatory tissue priming by metabolic reprogramming of synovial fibroblasts. *Immunity.* 2021; 54: 1002–1021.e10.
- [43] Dessauer CW, Chen-Goodspeed M, Chen J. Mechanism of Galpha i-mediated inhibition of type V adenylyl cyclase. *The Journal of Biological Chemistry.* 2002; 277: 28823–28829.
- [44] Morigi M, Perico L, Corna D, Locatelli M, Cassis P, Carminati CE, *et al.* C3a receptor blockade protects podocytes from injury in diabetic nephropathy. *JCI Insight.* 2020; 5: e131849.
- [45] Lim J, Iyer A, Suen JY, Seow V, Reid RC, Brown L, *et al.* C5aR and C3aR antagonists each inhibit diet-induced obesity, metabolic dysfunction, and adipocyte and macrophage signaling. *FASEB Journal: Official Publication of the Federation of American Societies for Experimental Biology.* 2013; 27: 822–831.
- [46] Seok S, Kim YC, Byun S, Choi S, Xiao Z, Iwamori N, *et al.* Fasting-induced JMJD3 histone demethylase epigenetically activates mitochondrial fatty acid  $\beta$ -oxidation. *The Journal of Clinical Investigation.* 2018; 128: 3144–3159.
- [47] Choung JS, Lee YS, Jun HS. Exendin-4 increases oxygen consumption and thermogenic gene expression in muscle cells. *Journal of Molecular Endocrinology.* 2017; 58: 79–90.
- [48] Gao S, Cui Z, Zhao MH. The Complement C3a and C3a Receptor Pathway in Kidney Diseases. *Frontiers in Immunology.* 2020; 11: 1875.
- [49] Peng Q, Li K, Smyth LA, Xing G, Wang N, Meader L, *et al.* C3a and C5a promote renal ischemia-reperfusion injury. *Journal of the American Society of Nephrology: JASN.* 2012; 23: 1474–1485.
- [50] Thurman JM, Lenderink AM, Royer PA, Coleman KE, Zhou J, Lambris JD, *et al.* C3a is required for the production of CXC chemokines by tubular epithelial cells after renal ischemia/reperfusion. *Journal of Immunology (Baltimore, Md.: 1950).* 2007; 178: 1819–1828.
- [51] Buelli S, Locatelli M, Carminati CE, Corna D, Cerullo D, Imberti B, *et al.* Shiga Toxin 2 Triggers C3a-Dependent Glomerular and Tubular Injury through Mitochondrial Dysfunction in Hemolytic Uremic Syndrome. *Cells.* 2022; 11: 1755.
- [52] You D, Weng M, Wu X, Nie K, Cui J, Chen Y, *et al.* C3aR contributes to unilateral ureteral obstruction-induced renal interstitial fibrosis via the activation of the NLRP3 inflammasome. *Life Sciences.* 2022; 308: 120905.
- [53] Zhang Y, Yan X, Zhao T, Xu Q, Peng Q, Hu R, *et al.* Targeting C3a/C5a receptors inhibits human mesangial cell proliferation and alleviates immunoglobulin A nephropathy in mice. *Clinical and Experimental Immunology.* 2017; 189: 60–70.
- [54] Zhang LY, Pan J, Mamtilahun M, Zhu Y, Wang L, Venkatesh A, *et al.* Microglia exacerbate white matter injury via complement C3/C3aR pathway after hypoperfusion. *Theranostics.* 2020; 10: 74–90.
- [55] Ito S, Hashimoto H, Yamakawa H, Kusumoto D, Akiba Y, Nakamura T, *et al.* The complement C3-complement factor D-C3a receptor signalling axis regulates cardiac remodelling in right ventricular failure. *Nature Communications.* 2022; 13: 5409.
- [56] Bao L, Osawe I, Haas M, Quigg RJ. Signaling through up-regulated C3a receptor is key to the development of experimental lupus nephritis. *Journal of Immunology (Baltimore, Md.: 1950).* 2005; 175: 1947–1955.
- [57] Lee A. Avacopan: First Approval. *Drugs.* 2022; 82: 79–85.
- [58] Müller DN, Derer W, Dechend R. Aliskiren—mode of action and preclinical data. *Journal of Molecular Medicine (Berlin, Germany).* 2008; 86: 659–662.
- [59] Li XX, Kumar V, Clark RJ, Lee JD, Woodruff TM. The “C3aR Antagonist” SB290157 is a Partial C5aR2 Agonist. *Frontiers in Pharmacology.* 2021; 11: 591398.
- [60] Atanes P, Ruz-Maldonado I, Pingitore A, Hawkes R, Liu B, Zhao M, *et al.* C3aR and C5aR1 act as key regulators of human and mouse  $\beta$ -cell function. *Cellular and Molecular Life Sciences: CMLS.* 2018; 75: 715–726.
- [61] Ishii M, Beeson G, Beeson C, Rohrer B. Mitochondrial C3a Receptor Activation in Oxidatively Stressed Epithelial Cells Reduces Mitochondrial Respiration and Metabolism. *Frontiers in Immunology.* 2021; 12: 628062.
- [62] Gao H, Neff TA, Guo RF, Speyer CL, Sarma JV, Tomlins S, *et al.* Evidence for a functional role of the second C5a receptor C5L2. *FASEB Journal: Official Publication of the Federation of American Societies for Experimental Biology.* 2005; 19: 1003–1005.
- [63] Zhang T, Wu KY, Ma N, Wei LL, Garstka M, Zhou W, *et al.* The C5a/C5aR2 axis promotes renal inflammation and tissue damage. *JCI Insight.* 2020; 5: e134081.
- [64] Martin IV, Bohner A, Boor P, Shagdarsuren E, Raffetseder U, Lammert F, *et al.* Complement C5a receptors C5L2 and C5aR in renal fibrosis. *American Journal of Physiology. Renal Physiology.* 2018; 314: F35–F46.
- [65] Hu C, Li L, Ding P, Li L, Ge X, Zheng L, *et al.* Complement Inhibitor CRIg/FH Ameliorates Renal Ischemia Reperfusion Injury via Activation of PI3K/AKT Signaling. *Journal of Immunology (Baltimore, Md.: 1950).* 2018; 201: 3717–3730.